Plant Physiology and Biochemistry 135 (2019) 167–173

Contents lists available at ScienceDirect

Plant Physiology and Biochemistry

journal homepage: www.elsevier.com/locate/plaphy

Research article

Overexpression of maize *MYB-IF35* increases chilling tolerance in Arabidopsis

Chen Meng[a], Na Sui[b,*]

[a] Marine Agriculture Research Center, Tobacco Research Institute of Chinese Academy of Agricultural Sciences, Qingdao, 266101, China
[b] Shandong Provincial Key Laboratory of Plant Stress, College of Life Sciences, Shandong Normal University, Jinan, 250014, China

ARTICLE INFO

Keywords:
Maize
ZmMYB-IF35
Chilling stress
Antioxidant enzymes

ABSTRACT

Chilling stress is a critical environmental factor that limits plant growth, yield and distribution. Maize (*Zea mays* L.) is an important food and forage crop, and industrial raw material, in China. Low temperatures can decrease maize production, especially in early spring. The R2R3-MYB transcription factor *ZmMYB-IF35* was isolated from maize cDNA. The open reading frame of *ZmMYB-IF35* is 1038 bp, encoding 345 amino acids with a molecular mass of 37.9 kDa. ZmMYB-IF35 localized in the nucleus. Low temperatures induced the expression of *ZmMYB-IF35* in maize, and the relative expression level reached its maximum after 4 h of chilling stress. The overexpression of *ZmMYB-IF35* under the control of the CaMV35S promoter in Arabidopsis conferred tolerance to chilling stress compared with the wild-type plants by maintaining the maximal photochemical efficiency of photosystem II. Furthermore, under chilling stress, the *ZmMYB-IF35* transgenic plants showed greater antioxidant enzyme activity levels, lower reactive oxygen species contents and lower ion leakage levels than those of wild-type plants. Thus, the overexpression of *ZmMYB-IF35* may enhance resistance to chilling and oxidative stresses in transgenic Arabidopsis and alleviates PSII photoinhibition.

1. Introduction

Chilling stress is an abiotic factor that limits plant growth, development, distribution and yield. During chilling stress, a number of major biological processes, such as photosynthesis, protein synthesis, lipid metabolism and secondary metabolism, are affected. The first component damaged by chilling stress is the chloroplast membrane. Chilling tolerance is related to the composition and structure of plant membrane lipids and their ability to transition from a liquid-crystalline phase to a gel phase. Tolerance to chilling stress is closely connected with the unsaturated fatty acid content of plant membrane lipids.

Low temperatures can affect all aspects of plant physiological metabolism. Photosynthesis is highly susceptible to low temperatures (Powles, 1984). Low temperature stress can affect many aspects of photosynthesis, including stomatal opening, photosynthetic electron transport rate, carbon assimilation and other processes. When the light energy absorbed by the photosynthetic mechanism exceeds the range that can be used, the photochemical efficiency of the system is reduced and photoinhibition is induced, which results in the decrease in the photosynthetic rate and photosystem II (PSII) photochemical efficiency (Fv/Fm). Under low temperature conditions, the decrease in the photosynthetic rate in plant leaves is related to the damage to the PSII reaction center and chloroplasts. Under long-term low-temperature stress conditions, membranes often suffer severe damage, resulting in a large accumulation of reactive oxygen species (ROS), severe PSII photoinhibition, and even light-related damage, which, to some extent, reduces the damage to photosystem I.

Under abiotic stress conditions, if excess light cannot be dissipated in time, or the carbon assimilation process is blocked, the accumulation of ROS, such as superoxide ($O_2^{-\cdot}$), singlet oxygen, hydrogen peroxide (H_2O_2) and hydroxyl radical is induced (Foyer and Shigeoka, 2011). The excessive accumulation of ROS causes a variety of serious injuries to plants (Singh and Singhal, 1999; Stepien and Klobus, 2005; Flowers and Colmer, 2008), such as damage to the proteins, carbohydrates, lipids and DNA, and even results in cell death (Mittler et al., 2004; Foyer and Noctor, 2005). Fortunately, plants have developed some protective mechanisms, including enzymatic and non-enzymatic antioxidant defense systems, to detoxify ROS and to protect themselves from oxidants. The non-enzymatic antioxidants include ascorbic acid, carotenoids, glutathione, tocopherols and flavonoids. Superoxide dismutase (SOD) is a major scavenger that defends against oxidative stress induced by superoxide in plant cells, and it plays a key role in scavenging $O_2^{-\cdot}$ to form H_2O_2. Ascorbate peroxidase (APX) plays important roles in protecting the component of chloroplasts and other cells from damage by

* Corresponding author.
E-mail address: suina800101@163.com (N. Sui).

https://doi.org/10.1016/j.plaphy.2018.11.038
Received 4 July 2018; Received in revised form 8 October 2018; Accepted 30 November 2018
Available online 07 December 2018
0981-9428/

H_2O_2 and the hydroxyl radicals. It converts H_2O_2 to water with ascorbic acid (AsA) as a specific electron donor and is involved in the most important pathway in H_2O_2 detoxification in chloroplasts (Foyer and Halliwell, 1976; Noctor and Foyer, 1998; Asada, 1999). Because more than 50% of APX in the chloroplasts is thylakoid bound, the membrane lipid transition from the liquid crystalline phase to gel phase during chilling stress can affect the activity level of thylakoid-bound APX and consequently affect ROS scavenging (Sonoike and Terashima, 1994).

Maize (*Zea mays* L.) is an important food and crop, as well as an industrial raw material, in China, playing important roles in agriculture and in the national economy. The accumulated temperature of the whole growth period is more than 10 °C. The optimum growth temperature is between 25 °C and 28 °C. When the temperature is lower than 12 °C, the plants are vulnerable to damage by chilling stress. Low temperatures can decrease maize production by affecting seed germination and seedling growth, especially during early spring. However, the mechanism of chilling tolerance in maize is still unknown. In this study, the important *ZmMYB-IF35* gene, which is involved in chilling tolerance in maize, was screened, and its function during chilling stress was investigated. The results provide valuable information to increase our understanding of the mechanisms of chilling tolerance in maize.

2. Materials and methods

2.1. Plant materials and growth conditions

In the previous experiment, 102 maize inbred lines were used for chilling tolerance determination, and a chilling tolerant line, M54, and a chilling sensitive line, 753F, were selected for RNA-seq analyses. In this experiment, seeds of maize inbred line M54 (chilling tolerant) were used. Dry seeds were stored in a refrigerator at 4 °C before use. Maize seeds of uniform size were selected and soaked in water for 10 h. Plants were grown at 30/22 °C (day/night), with a 14-/10-h (light/dark) photoperiod and light intensity of $\sim 400 \pm 50\ \mu mol\ m^{-2}\ s^{-1}$. The relative humidity levels were 60% and 70% during the day and night, respectively.

Arabidopsis 'Columbia-0' was selected as the wild-type (WT) control. Arabidopsis seeds were grown at 22/18 °C (day/night) under a 16-/8-h (light/dark) photoperiod. Two weeks later, the plants were treated with chilling stress (4 °C) for 3, 6, 9 and 12 h to determine the physiological indices.

2.2. Cloning and sequencing of MYB-IF35, and its transformation into Arabidopsis

From the RNA-seq data, the gene of *MYB-IF35* which was up-regulated only in M54 was selected in this experiment. Total RNA was extracted with TRIzol reagent according to the manufacturer's instructions. Gene-specific primers (forward: 5′-ATGGGGAGGGCGCCGTGC-3′ and reverse: 5′-GAGATTGTCCAGGAAGAAGAGG-3′) were used to amplify the full length of *MYB-IF35*. The full-length open reading frame of *MYB-IF35* was inserted into the plant binary vector pROKII to construct pROKII–MYB-IF35. Then, the *MYB-IF35* gene controlled by the CaMV35S promoter was transformed into Arabidopsis using the *Agrobacterium tumefaciens*-mediated transformation method (Zhang et al., 2006; Sui et al., 2017), and the T3 generation was used for further analysis.

2.3. Bioinformatics analysis of MYB-IF35

The BLASTp online tool and DNAMAN software were used to analyze the phylogenetic relationships, based on the amino acid sequences, of *ZmMYB-IF35* with *MYB-IF35* genes from other plant species.

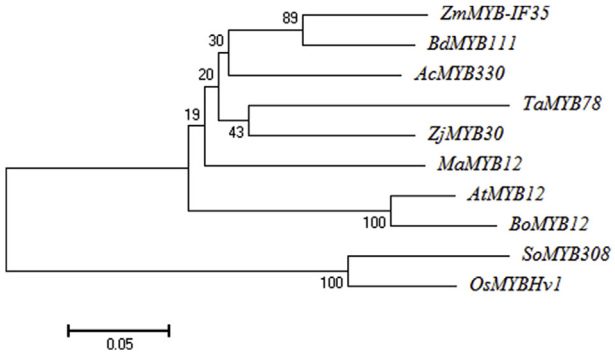

Fig. 1. Phylogenetic relationships among amino acid residue sequences of the conserved cyclin-box domains of maize *ZmMYB-IF35* and *MYB-IF35* genes from *Oryza sativa* (*Japonica* group), *Brachypodium distachyum*, *Sorghum bicolor*, *Triticum aestivum*, *Arabidopsis thaliana*, *Brassica oleracea* var. *Oleracea*, *Hordeum vulgare* and *Echinochloa crus-galli*.

2.4. Quantitative real-time PCR analysis

The expression profile of *ZmMYB-IF35* in maize leaves under chilling stress (4 °C) for 0, 4, 12 and 24 h was investigated using forward (5′-CTTGGCAACAGGTGGTCC-3′) and reverse (5′-GGTGCGAGTTCCAGT AGTT-3′) primers. *ZmMYB-IF35* was also overexpressed in Arabidopsis lines. Amplification of the ACTIN gene was used as an internal control, and the primer pairs used for the analysis were ZmActin-F (5′-GGAGC TCGAGAATGCCAAGAGCAG-3′) and ZmActin-R (5′-GACCTCAGGGCA TCTGAACCTCTC-3′), and AtActin2 (5′-AAGCTGGGGTTTTATGAA TGG-3′) and AtActin2 (5′-TTGTCACACACAAGTGCATCAT-3′), which were designed according to the ACTIN nucleotide sequences of maize and Arabidopsis, respectively.

2.5. The subcellular localization of MYB-IF35

The full length of *ZmMYB-IF35* was generated by PCR and then cloned into the pROKII-GFP vector using forward (5′-CGAGCTCATGG GGAGGGCGCCGTGC-3′) and reverse (5′-CGGGATCCGAGATTGTCCAG GAAGAAGAGG-3′) primers. The pROKII-GFP-ZmMYB-IF35 transient vector was successfully constructed and transformed into *A. tumefaciens* 'EHA105'. Tobacco epidermal cells were then infected, and fluorescence microscopy was used to determine the subcellular localization of the *ZmMYB-IF35* protein.

2.6. Determinations of minimal fluorescence (Fo) and maximal photochemical efficiency (Fv/Fm)

Chl fluorescence was determined according to our previous method (Yang et al., 2013; Cheng et al., 2014) using a portable fluorometer (FMS2; Hansatech, King's Lynn, UK). The Fo with all PSII reaction centers open was determined by modulated light that was low enough not to induce any significant variable fluorescence (Fv). Maximal fluorescence (Fm) with all reaction centers closed was determined by 0.8 s saturating light of $8000\ \mu mol\ m^{-2}\ s^{-1}$ on a dark-adapted leaf (adapted 30 min in darkness). The Fv/Fm of PSII was expressed as: Fv/Fm = (Fm – Fo)/Fm.

2.7. Determinations of the antioxidant enzyme activity levels, and $O_2^{-\cdot}$ and H_2O_2 contents

Ascorbate peroxidase (APX) activity was determined according to our previous method (Sui, 2015) by measuring the decreased absorbance at 290 nm. Enzyme activity was calculated per mg of total protein in U, which represents the amount of enzyme needed to oxide 1 μmol of AsA within 1 min at room temperature.

Superoxide dismutase (SOD) activity was determined according to

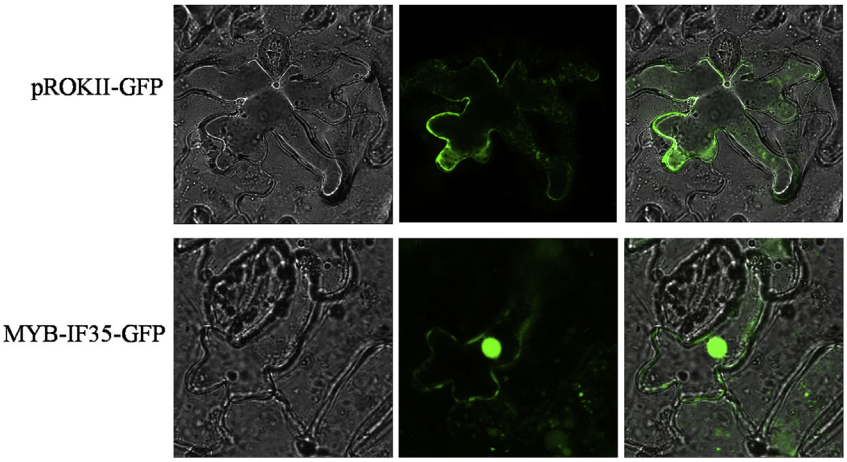

Fig. 2. Subcellular localization of *ZmMYB-IF35* in tobacco epidermal cells. Transient expression vectors p35S:*ZmMYB-IF35*-GFP and p35S:GFP were constructed and independently transformed into tobacco epidermal cells. Green fluorescence was observed under a differential interference contrast microscope 3 d after transformation. (For interpretation of the references to color in this figure legend, the reader is referred to the Web version of this article.)

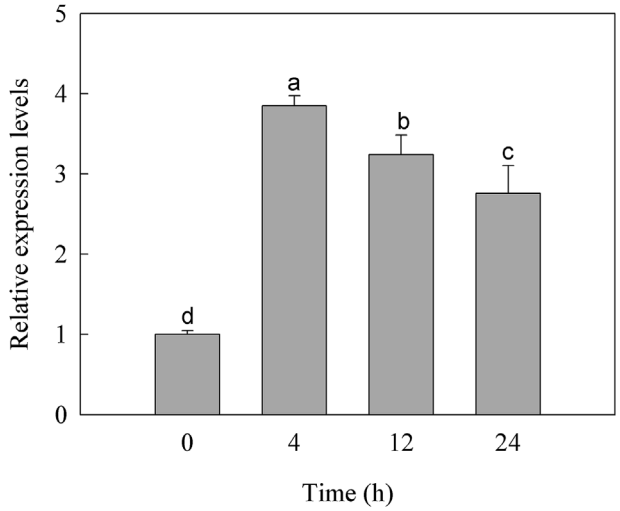

Fig. 3. Relative expression levels of *ZmMYB-IF35* in maize. Total RNA was isolated from maize leaves, and the expression levels were normalized to maize Actin. Seedlings were subjected to chilling stress (4 °C) for 0, 4, 12 and 24 h. Data were expressed as means ± SDs of five measurements (n = 5). Means identified by different lowercase letters are significantly different at $P \leq 0.05$.

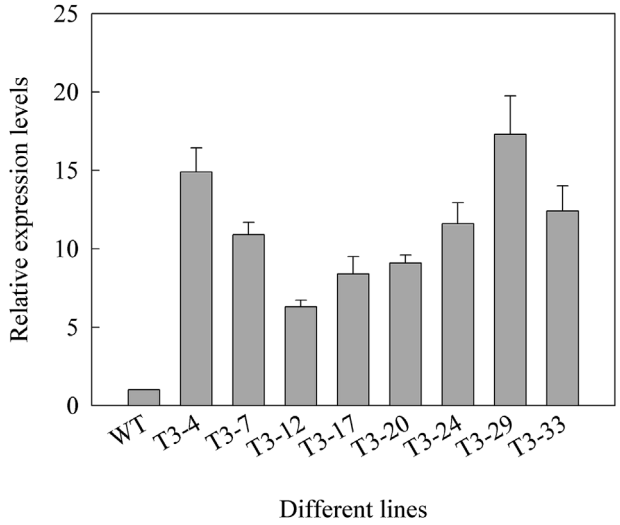

Fig. 4. Relative expression levels of different *ZmMYB-IF35*-overexpression Arabidopsis lines. Total RNA was isolated from Arabidopsis leaves, and the expression levels were normalized to Arabidopsis Actin. Data were expressed as means ± SDs of five measurements (n = 5).

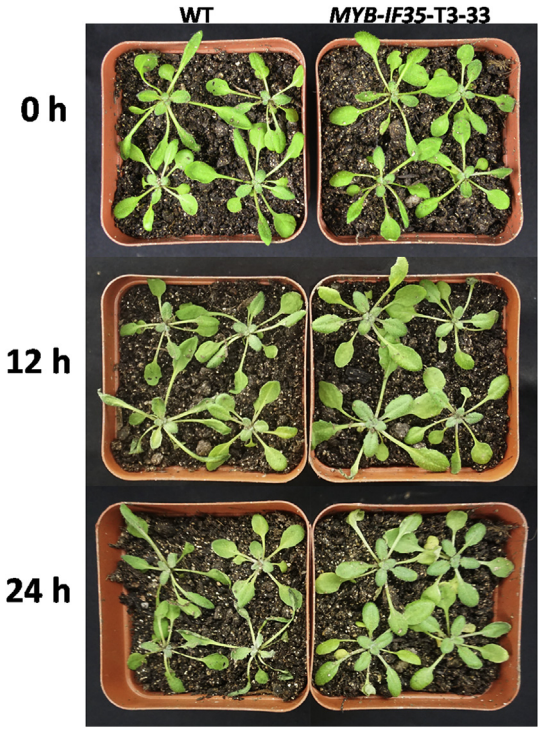

Fig. 5. Phenotypes of the wild-type (WT) and a transgenic Arabidopsis line (T3-33) subjected to chilling stress for 0, 12 and 24 h.

the method of Giannopolitis and Ries. Enzyme activity was calculated as 50% inhibition, expressed in U per mg of total protein, by measuring the absorbance at 560 nm using a UV/Vis spectrophotometer (UV-1601; Shimadzu, Kyoto, Japan).

The $O_2^{-\cdot}$ content was analyzed according to the method introduced in our previous study (Liu et al., 2017). The $O_2^{-\cdot}$ generated, presented as per g fresh mass of leaves, was determined by measuring the absorbance at 530 nm using the water phase.

Elicitation of $O_2^{-\cdot}$ can be *In situ* detected by nitroblue tetrazolium (NBT) according to the method of Buapet and Björk (2016).

The H_2O_2 content was determined according to the method introduced in our previous study (Sui et al., 2018) by measuring the absorbance of the titanium–hydroperoxide complex and a standard curve plotted was used in the determination.

Elicitation of H_2O_2 can be *In situ* detected by 3,3′-diaminobenzidine (DAB) staining according to the method of Thordal-Christensen et al. (1997).

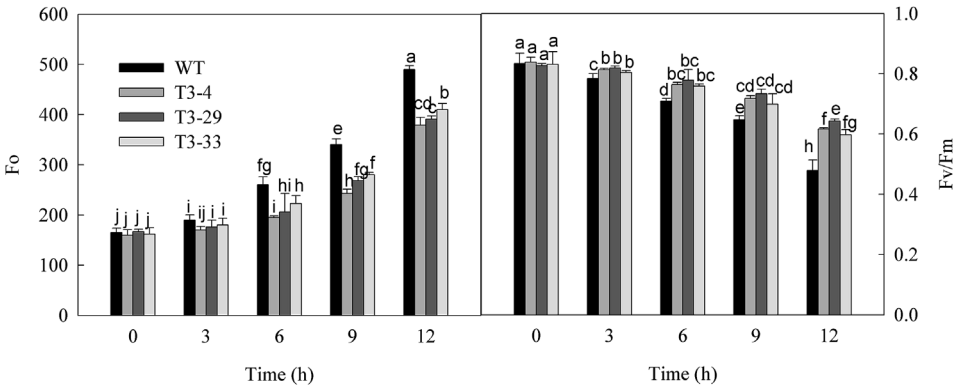

Fig. 6. Effects of chilling stress (4 °C) on the Fo and Fv/Fm in leaves of WT Arabidopsis and *ZmMYB-IF35*-overexpression lines. The Fo and Fv/Fm were measured during 0-, 3-, 6-, 9- and 12-h chilling treatments. Values are means ± SDs of five measurements (n = 5). Means identified by different lowercase letters are significantly different at $P \leq 0.05$.

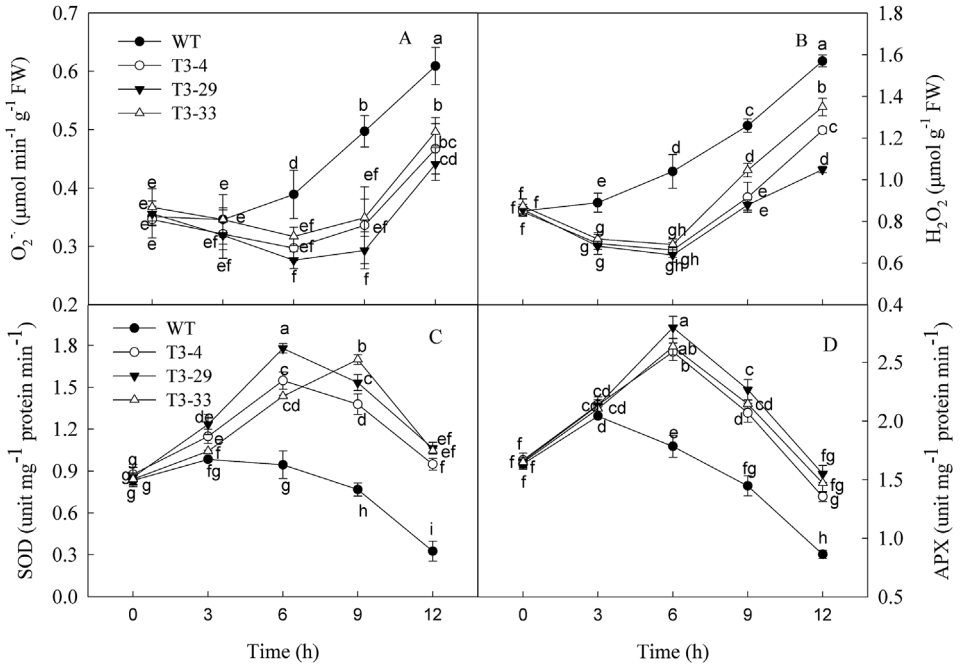

Fig. 7. Changes in the $O_2^{\cdot-}$ (A) and H_2O_2 (B) contents and the SOD (C) and APX (D) activities of WT Arabidopsis and *ZmMYB-IF35*-overexpression lines after being subjected to chilling stress (4 °C) for 0, 3, 6, 9 and 12 h. Data are means ± SDs of five replicates (n = 5). Means identified by different lowercase letters are significantly different at $P \leq 0.05$.

2.8. Determination of relative electronic conductance (REC)

The REC was determined according to our previous method (Zhou et al., 2016). In total, 40 leaf disks (1 cm^2 each) were placed in a cuvette containing 20 mL distilled water, placed in a vacuum for 30 min, and then subjected to an electrical surge for 4 h to measure the initial electronic conductance (S1). The cuvette was heated in boiling water for 30 min and cooled to room temperature to determine the final electronic conductance (S2). The REC was evaluated as follows: REC = (S1/S2) × 100.

2.9. Statistical analyses

Statistical analyses were performed to ensure the homogeneity of variance. All tests were performed with SPSS Version 19.0 for Windows (SPSS, Chicago. IL, USA). Multiple comparisons between different treatments were performed using Duncan's multiple range test at the 0.05 significance level.

3. Results

3.1. Sequence analysis of ZmMYB-IF35

The open reading frame of *ZmMYB-IF35* of maize is 1038 bp, which encodes 345 amino acids with a molecular mass of 37.9 kDa. To investigate the evolutionary relationships between maize ZmMYB-IF35 and MYB-IF35s from other plants, a phylogenetic tree of the conserved cyclin-box domains was constructed. Maize MYB-IF35 shared the highest identity with MYB-IF35 from *Sorghum bicolor* (Fig. 1).

3.2. Subcellular localization of ZmMYB-IF35

To check the subcellular localization of ZmMYB-IF35, the recombinant pROKII-GFP-ZmMYB-IF35 fusion vector and the pROKII-GFP vector alone were independently transformed into tobacco epidermal cells through *Agrobacterium* infection. The GFP alone was expressed throughout the whole cell, while the pROKII-GFP-ZmMYB-IF35 fusion protein accumulated mainly in the nucleus (Fig. 2). This suggests that ZmMYB-IF35 is a nuclear-localized protein.

3.3. Chilling induces the expression of ZmMYB-IF35 in maize

To determine whether the expression of *ZmMYB-IF35* was induced by chilling stress, the relative expression level of *ZmMYB-IF35* in maize under chilling stress for 0, 4, 12 and 24 h was determined by quantitative real-time PCR (qPCR). As shown in Fig. 3, the relative expression level of *ZmMYB-IF35* reached its maximum level after 4 h of chilling stress, and declined slightly thereafter.

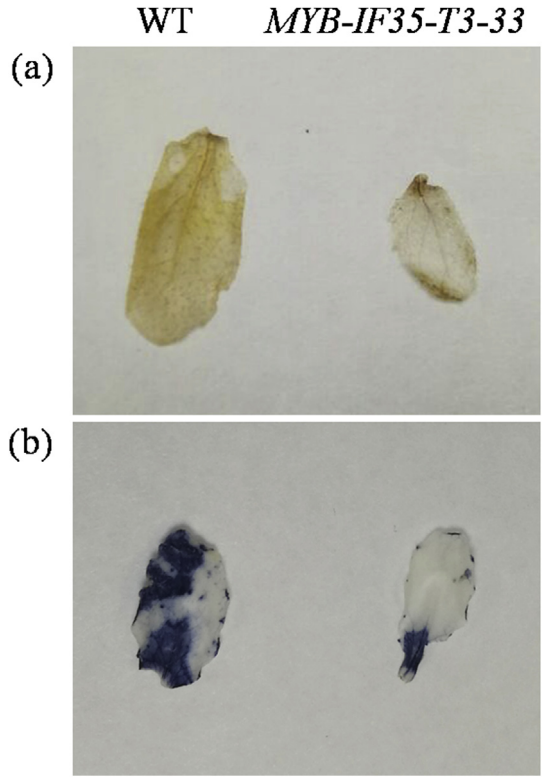

Fig. 8. *In situ* detection of $O_2^{-\cdot}$ by nitroblue tetrazolium (NBT) (a) and H_2O_2 by 3,3′-diaminobenzidine (DAB) staining (b).

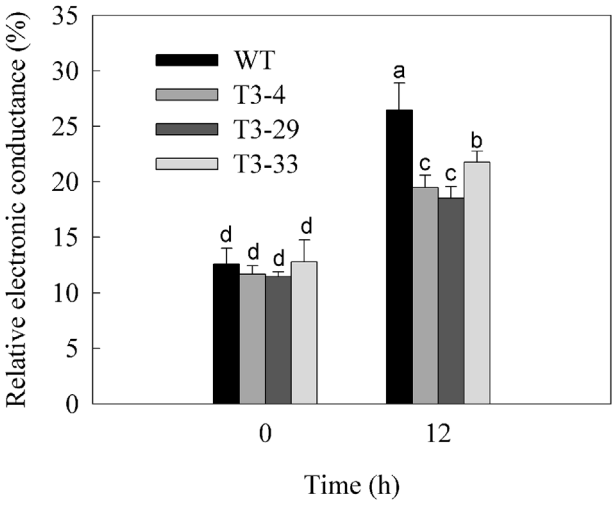

Fig. 9. Effects on the relative electronic conductance of WT Arabidopsis and *ZmMYB-IF35*-overexpression lines after being treated with chilling stress (4 °C) for 0 and 12 h. Data are means ± SDs of five replicates (n = 5). Means identified by different lowercase letters are significantly different at $P \leq 0.05$.

3.4. *ZmMYB-IF35 overexpressing Arabidopsis lines*

To understand the role of *ZmMYB-IF35* in the plant abiotic stress responses, we overexpressed *ZmMYB-IF35* in Arabidopsis under the control of the CaMV 35S promoter. The expression of *ZmMYB-IF35* at the transcriptional level was examined, and three T3 homozygous transgenic lines (T3-4, T3-29 and T3-33), which exhibited relatively high expression levels, were selected (Fig. 4).

3.5. *Overexpression of ZmMYB-IF35 enhances the chilling tolerance of Arabidopsis*

As shown in Fig. 5, after being treated with chilling stress for 12 and 24 h, the leaves of the WT and Arabidopsis *ZmMYB-IF35*-overexpression line T3-33 wilted and yellowed; however, the response was more severe in WT than in 'T3-33' (Fig. 5).

There were no significant differences in Fo and Fv/Fm values among the WT, T3-4, T3-29 and T3-33 lines (Fig. 6). However, during a low-temperature treatment, the Fo of the WT, T3-4, T3-29 and T3-33 lines significantly increased compared with that of the control, whereas the Fv/Fm decreased under chilling stress (Fig. 6). After being treated at 4 °C for 12 h, the Fo of WT, T3-4, T3-29 and T3-33 lines increased by 197%, 137%, 134% and 153%, respectively; while the Fv/Fm of the WT, T3-4, T3-29 and T3-33 lines decreased by 42.6%, 26.6%, 22.2% and 28.1%, respectively.

No differences in the $O_2^{-\cdot}$ and H_2O_2 contents were observed between the WT and transgenic plants under normal conditions. The $O_2^{-\cdot}$ and H_2O_2 contents of WT and transgenic plants initially decreased and then increased (Fig. 7A and B). During the chilling treatment, the $O_2^{-\cdot}$ and H_2O_2 contents of the WT were greater than those of transgenic plants. After being treated for 12 h, the $O_2^{-\cdot}$ contents of the WT, T3-4, T3-29 and T3-33 lines increased by 73.5%, 35.0%, 23.9% and 35.1%, respectively; while the H_2O_2 contents of the WT, T3-4, T3-29 and T3-33 lines increased by 84.7%, 46.2%, 22.4% and 54.5%, respectively. The degree of NBT and DAB staining was also higher in WT than in transgenic plants (Fig. 8).

There were no differences in SOD and APX activity levels between WT and transgenic plants under normal conditions. However, the SOD and APX activity levels of the transgenic plants were greater than those of WT during the chilling treatment (Fig. 7C and D). SOD and APX activity levels in WT and transgenic plants initially increased and then decreased under chilling stress. After being treated for 12 h, the SOD activity of the WT decreased by 60.9%, while the SOD activities of the T3-4, T3-29 and T3-33 lines increased by 8.2%, 24.2% and 24.3%, respectively. The APX activities of the WT, T3-4, T3-29 and T3-33 lines decreased by 47.2%, 18.7%, 6.5% and 10.7%, respectively.

Under normal conditions, there were no significant differences in REC between WT and transgenic plants (Fig. 9). However, the REC values of the T3-4, T3-29 and T3-33 lines were lower than that of WT during the 12-h 4 °C treatment (Fig. 9). The REC values of the WT, T3-4, T3-29 and T3-33 lines increased by 110%, 66.6%, 61.4% and 70.1%, respectively.

3.6. *Expression of chilling stress-related genes in WT and transgenic lines*

We determined the expression patterns of some chilling stress-related genes (*AtCBF2*, *AtCBF3*, *AtCOR1* and *AtCOR2*) in WT and transgenic lines to evaluate the molecular regulatory mechanism of *ZmMYB-IF35*. The expression level of these genes were all greater in the transgenic lines than in WT under both control and chilling-treated condition (Fig. 10). Thus, the overexpression of *ZmMYB-IF35* affected the expression of chilling stress-related genes.

4. Discussion

Low temperature is an important factor that limits the distribution, yield and quality of plants. Maize is one of the most popular crop species worldwide, and its optimum growth temperature is between 25 °C and 28 °C. When the temperature is below 12 °C, corn plants are vulnerable to damage by chilling stress. Thus, it is important to improve the chilling tolerance of maize using transgenic technology.

In the present study, the cDNA of *ZmMYB-IF35*, which encodes a protein of 345 amino acids, was isolated from maize and transformed into Arabidopsis plants under the control of the 35S-CaMV promoter. An amino acid sequence analysis showed that ZmMYB-IF35 had the

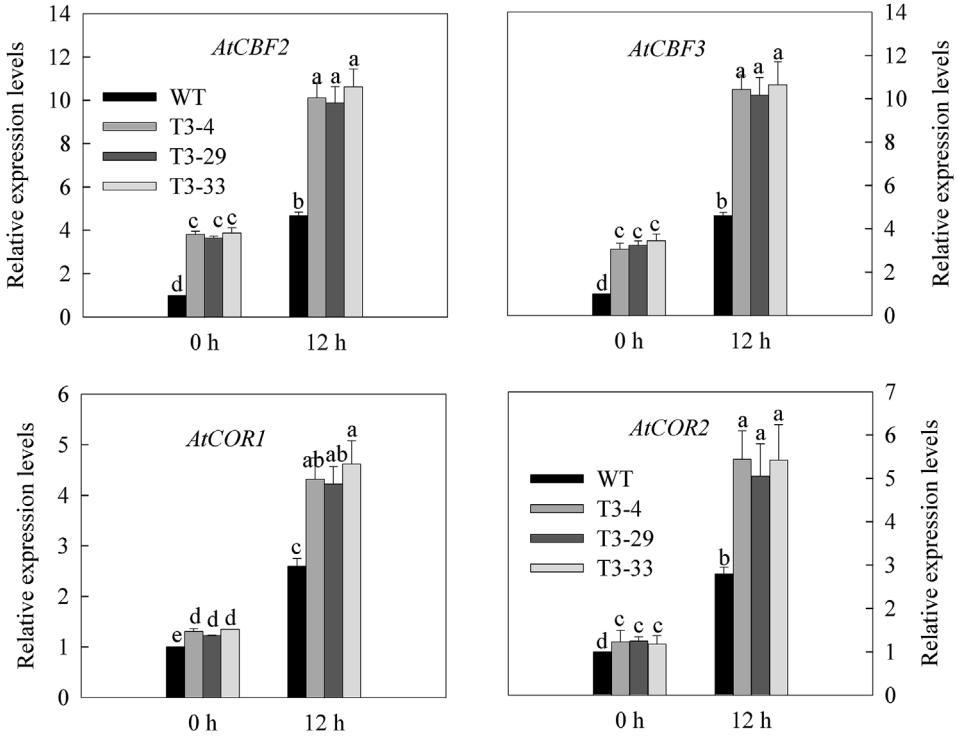

Fig. 10. Expressions levels of some marker genes (*AtCBF2*, *AtCBF3*, *AtCOR1* and *AtCOR2*) under chilling stress in WT Arabidopsis and *ZmMYB-IF35*-overexpression lines. Data are means ± SDs of five replicates (n = 5). Means identified by different lowercase letters are significantly different at $P \leq 0.05$.

greatest homology with MYB-IF35 proteins from *Sorghum bicolor* (Fig. 1). We have determined that ZmMYB-IF35 localizes to the nucleus (Fig. 2). An analysis of *ZmMYB-IF35* transcripts in the leaves of maize subjected to a chilling stress for different time periods showed that the greatest transcript level was attained at 4 h of chilling stress (Fig. 3). This suggests that the transcription of maize *ZmMYB-IF35* can be induced by a low temperature. We screened and identified Arabidopsis overexpression lines, in which the expression levels of *ZmMYB-IF35* were much greater than that in WT (Fig. 4). Three T3 homozygous transgenic lines (T3-4, T3-29 and T3-33) that exhibited relatively high expression levels were selected for further study.

Chilling stress inhibits leaf photosynthesis through PSII-related photoinhibition (Aro et al., 1993; Zhang et al., 2011). PSII is believed to play an important role in plant responses to environmental stresses (Baker, 1991; Sui and Han, 2014). However, the PSII activity level, which is reflected by Fv/Fm, was not affected in WT and transgenic plants under normal conditions (Fig. 6). The Fv/Fm decreased in both WT and transgenic plants during chilling stress, but especially in the former. This suggests that *ZmMYB-IF35* overexpression can protect PSII during chilling stress. Changes in the Fo depend on the factors present during energy dissipation and PSII inactivation (Guo et al., 2018). PSII damage or inactivation can result in an increase in Fo (Xu and Wu, 1996). In this study, the Fo increased during chilling stress; however, the increase was smaller in transgenic plants than in WT (Fig. 6), which indicated less damage to the PSII of transgenic plants than that of WT. Thus, the overexpression of maize *ZmMYB-IF35* could alleviate damage caused by chilling stress to photosynthetic reaction centers and reduce chilling photoinhibition.

If the excess energy absorbed by plants cannot be dissipated in time, or the CO_2 assimilation is blocked, ROS is generated, especially under conditions of environmental stress (Asada, 1992, 1999), and ROS can affect the membrane integrity, aggravate membrane lipid peroxidation and cause plant damage (Smirnoff, 1993; Mehdy, 1994). During evolution, many mechanisms for scavenging ROS were generated in plants, including various nonenzymatic and enzymatic antioxidants, as APX, SOD and catalase (Song et al., 2005). These can scavenge ROS and protect plants from ROS damage (Noctor and Foyer, 1998; Song et al., 2005; Airaki et al., 2012; Liu et al., 2017). Under normal conditions, there were no differences in $O_2^{-\cdot}$ and H_2O_2 contents between the WT and transgenic plants (Fig. 7A and B). However, under chilling stress, the $O_2^{-\cdot}$ and H_2O_2 contents of transgenic plants were lower than those of WT. SOD activity is crucial for the enzymatic scavenging of $O_2^{-\cdot}$ to form H_2O_2. APX is an important enzyme for eliminating toxic H_2O_2 in plants, and it can scavenge peroxides by converting AsA to dehydroascorbate (Foyer et al., 1994). Under chilling stress, SOD and APX activity levels initially increased and then decreased. In transgenic plants, the SOD and APX activities were greater than those of WT under chilling stress (Fig. 7C and D). The greater SOD and APX activity levels in transgenic plants allows more scavenging of $O_2^{-\cdot}$ and H_2O_2. Thus, the overexpression of maize *ZmMYB-IF35* could increase the activity levels of SOD and APX, which could effectively reduce $O_2^{-\cdot}$ and H_2O_2 contents, and reduce ROS damage to plants.

Chilling stress can affect plasma membrane permeability, which is the rate of passive diffusion of molecules through the membrane (Wang et al., 2014). The REC reflects the degree of membrane permeability. A greater REC value indicates an increase in permeability. In the present study, the REC increased in WT and transgenic plants under chilling stress (Fig. 9). However, it was greater in WT than in transgenic plants. Thus, the membranes may be more severely damaged in WT Arabidopsis than in transgenic plants. The overexpression of maize *ZmMYB-IF35* delays the REC increase.

In summary, the overexpression of maize *ZmMYB-IF35* alleviated the PSII photoinhibition, increased plant tolerance to chilling stress and increased the activity levels of SOD and APX, which can effectively scavenge ROS, reduce ion leakage and protect the photosynthetic apparatus from chilling damage. *ZmMYB-IF35* can also regulate the expression of stress-related genes in response to chilling stress. This study provides useful information that increases our understanding of the regulatory mechanisms of MYB transcription factors.

CRediT authorship contribution statement

Chen Meng: Writing – original draft, Investigation, Formal analysis, Writing – original draft. **Na Sui:** Conceptualization, Supervision, Writing – review & editing.

Acknowledgements

We are grateful for financial support from Major Program of Shandong Provincial Natural Science Foundation (2017C03), Shandong Natural Science Foundation (ZR2016JL028), the Doctor Foundation of Shandong (ZR2017BCE006), the Natural Science Foundation of China (31701339). We thank Lesley Benyon, PhD, from Liwen Bianji, Edanz Group China (www.liwenbianji.cn/ac), for editing the English text of a draft of this manuscript.

References

Airaki, M., Leterrier, M., Mateos, R.,M., Valderrama, R., Chaki, M., Barroso, J.,B.,, Del Rio, L.A., Palma, J.M., Corpas, F.J., 2012. Metabolism of reactive oxygen species and reactive nitrogen species in pepper (*Capsicum annuum* L.) plants under low temperature stress. Plant Cell Environ. 35, 281–295.

Aro, E., Virgin, I., Andersson, B., 1993. Photoinhibition of photosystem II. Inactivation, protein damage and turnover. Biochim. Biophys. Acta Bioenerg. 1143, 113–134.

Asada, K., 1999. The water-water cycle in chloroplasts: scavenging of active oxygens and dissipation of excess photons. Annu. Rev. Plant Biol. 1, 601–639.

Asada, K., 1992. Ascorbate peroxidase a hydrogen peroxide scavenging enzyme in plants. Physiol. Plantarum 85, 235–241.

Baker, N.R., 1991. A possible role for photosystem II in environmental perturbations of photosynthesis. Physiol. Plantarum 81, 563–570.

Buapet, P., Björk, M., 2016. The role of O_2 as an electron acceptor alternative to CO_2 in photosynthesis of the common marine angiosperm *Zostera marina* L. Photosynth. Res. 129 (1), 59–69.

Cheng, S., Yang, Z., Wang, M.J., Song, J., Sui, N., Fan, H., 2014. Salinity improves chilling resistance in Suaeda salsa. Acta Physiol. Plant. 36 (7), 1823–1830.

Flowers, T.J., Colmer, T.D., 2008. Salinity tolerance in halophytes. New Phytol. 179, 945–963.

Foyer, C.H., Halliwell, B., 1976. The presence of glutathione and glutathione reductase in chloroplasts: a proposed role in ascorbic acid metabolism. Planta 1, 21–25.

Foyer, C.H., Lelandais, M., Kunert, K.J., 1994. Photooxidative stress in plants. Physiol. Plantarum 92, 696–717.

Foyer, C.H., Noctor, G., 2005. Redox homeostasis and antioxidant signalling: a metabolic interface between stress perception and physiological responses. Plant Cell 17, 1866–1875.

Foyer, C.H., Shigeoka, S., 2011. Understanding oxidative stress and antioxidant functions to enhance photosynthesis. Plant Physiol. 155, 93–100.

Guo, Y.Y., Tian, S.S., Liu, S.S., et al., 2018. Energy dissipation and antioxidant enzyme system protect photosystem II of sweet sorghum under drought stress. Photosynthetica 1–12.

Liu, S., Wang, W., Li, M., et al., 2017. Antioxidants and unsaturated fatty acids are involved in salt tolerance in peanut. Acta Physiol. Plant. 39 (9), 207.

Mehdy, M.C., 1994. Active oxygen species in plant defense against pathogens. Plant Physiol. 105, 467–472.

Mittler, R., Vanderauwera, S., Gollery, M., van Breusegem, F., 2004. The reactive oxygen gene network of plants. Trends Plant Sci. 9, 490–498.

Noctor, G., Foyer, C.H., 1998. Ascorbate and glutathione: keeping active oxygen under control. Annu. Rev. Plant Biol. 49, 249–279.

Powles, S.B., 1984. Photoinhibition of photosynthesis induced by visible light. Annu. Rev. Plant Physiol. 35, 15–44.

Singh, A.K., Singhal, G.S., 1999. Specific degradation of D1 protein during exposure of thylakoid membranes to high temperature in dark. Photosynthetica 36, 433–440.

Smirnoff, N., 1993. The role of active oxygen in the response of plants to water deficit and desiccation. New Phytol. 125, 27–58.

Song, X.S., Hu, W.H., Mao, W.H., Ogweno, J.O., Zhou, Y.H., Yu, J.Q., 2005. Response of ascorbate peroxidase isoenzymes and ascorbate regeneration system to abiotic stresses in *Cucumis sativus* L. Plant Physiol. Biochem. 43, 1082–1088.

Sonoike, K., Terashima, I., 1994. Mechanism of photosystem-I photoinhibition in leaves of *Cucumis sativus* L. Planta 2, 287–293.

Stepien, P., Klobus, G., 2005. Antioxidant defense in the leaves of C3 and C4 plants under salinity stress. Physiol. Plantarum 125, 31–40.

Sui, N., Han, G.L., 2014. Salt-induced photoinhibition of PSII is alleviated in halophyte Thellungiella halophila by increases of unsaturated fatty acids in membrane lipids. Acta Physiol. Plant. 36, 983–992.

Sui, N., Wang, Y., Liu, S., et al., 2018. Transcriptomic and physiological evidence for the relationship between unsaturated fatty acid and salt stress in peanut. Front. Plant Sci. 9, 7.

Sui, N., Tian, S., Wang, W., et al., 2017. Overexpression of glycerol-3-phosphate acyltransferase from Suaeda salsa improves salt tolerance in Arabidopsis. Front. Plant Sci. 8, 1337.

Sui, N., 2015. Photoinhibition of Suaeda salsa to chilling stress is related to energy dissipation and water-water cycle. Photosynthetica 53 (2), 207–212.

Thordal-Christensen, H., Zhang, Z., Wei, Y., Collinge, D.B., 1997. Subcellular localization of H_2O_2 in plants. H_2O_2 accumulation in papillae and hypersensitive response during the barley-powdery mildew interaction. Plant J. 11, 1187–1194.

Wang, L., Meng, X., Yang, D., et al., 2014. Overexpression of tomato GDP-L-galactose phosphorylase gene in tobacco improves tolerance to chilling stress. Plant Cell Rep. 33 (9), 1441–1451.

Xu, D.Q., Wu, S., 1996. Three phases of dark-recovery course from photoinhibition resolved by the chlorophyll fluorescence analysis in soybean leaves under field conditions. Photosynthetica 32, 417–423.

Yang, J.C., Li, M., Xie, X.Z., et al., 2013. Deficiency of phytochrome B alleviates chilling-induced photoinhibition in rice. Am. J. Bot. 100 (9), 1860–1870.

Zhang, X., Henriques, R., Lin, S.S., Niu, Q.W., Chua, N.H., 2006. Agrobacterium-mediated transformation of Arabidopsis thaliana using the floral dip method. Nat. Protoc. 1, 641–646.

Zhang, Y.J., Yang, J.S., Guo, S.J., et al., 2011. Over-expression of the Arabidopsis cbf1 gene improves resistance of tomato leaves to low temperature under low irradiance. Plant Biol. 2, 362–367.

Zhou, J.C., Fu, T.T., Sui, N., et al., 2016. The role of salinity in seed maturation of the euhalophyte Suaeda salsa. Plant Biosyst. 150 (1), 83–90.